Environment, Resource and Ecology Journal (2023)
Clausius Scientific Press, Canada

DOI: 10.23977/erej.2023.070401
ISSN 2616-3756 Vol. 7 Num. 4

Soil Moisture Dynamics and the Response to Precipitation in Fixed Sand Dunes of Artemisia Ordosica Community in Mu Us Sandy Land

Liang Xianghan[1]

[1]*Management Committee of Beijing Olympic Park Central Area, Beijing, 100101, China*

Keywords: Precipitation; soil moisture; infiltration; Mu Us Sandy Land

Abstract: In order to deeply study the response of soil moisture to precipitation, the characteristics of precipitation infiltration and the recharge of precipitation to soil moisture in the fixed sand dunes of Artemisia Ordosica in Mu Us sandy land, this study used the AR-5 automatic soil moisture monitoring system and AV-3665R rainfall sensor to conduct long-term and continuous monitoring of soil moisture and precipitation in the fixed sand dunes of Artemisia Ordosica, and fitted the precipitation infiltration through the multi-compartment model. The results show that: (1) The accumulated precipitation in the growing season in the study area is 332.75 mm, which has a significant impact on the soil water content of 0-120 cm soil layer. The precipitation before August only affects 80 cm and above; The precipitation from August to October has a significant impact on the soil water content of 0-120cm soil layer. (2) After each precipitation event, the soil water content of 0-60 cm layer in various fields will change significantly. After each precipitation, the maximum water content of surface soil is significantly higher than that of deep soil. Since the initial soil water content before the second precipitation is significantly different, the maximum soil water content after the second precipitation is significantly higher than that after the first precipitation. The initial soil water content has a significant impact on infiltration and redistribution, which will make a significant difference between the migration rate of the wetting front and the maximum soil water content after precipitation. (3) The multi-compartment model is used to simulate the infiltration of precipitation, and the parameters are modified after the preliminary validation of the model. The results show that the modified model parameters meet the set value range, and the goodness of fit meets the statistical requirements. The modified model can better reflect the infiltration of different precipitation, different precipitation intensity, and different areas. According to the different range of parameters in the improved model, it can express the relationship between plants and soil moisture under different precipitation conditions and different time periods.

Mu Us sandy land is located in the area where semi desert and Forest steppe interact, and its soil and vegetation have transitional characteristics [1-5]. Artemisia ordosica is one of the local constructive and dominant species, with 29.9% of the sandy area being the Artemisia ordosica community, which is significantly larger than other types of sandy plants. Artemisia annua has

strong resistance and stability to arid and windy environments, and plays a crucial role in the stability of local ecosystems. Existing studies have shown that the natural succession of Artemisia annua communities is a cyclic process of vegetation coverage from small to large, and then from large to small, with soil moisture being the main driving force behind this process and playing an irreplaceable role. Soil water refers to the water in the soil layer from the surface of the soil to the surface of the groundwater table [6-9]. It is an important component of water resources in desert ecosystems and serves as a bridge connecting precipitation, surface water, atmospheric water, and groundwater. In arid and semi-arid regions, soil moisture seriously restricts the growth and development of plants, and land degradation is directly related to the decrease in soil moisture content. Therefore, research on soil moisture is of great significance for local sustainable development and rational utilization of vegetation [10-14].

Previously, scholars have conducted some research on the relationship between rainfall and soil moisture in the Mu Us sandy land, and preliminarily obtained the characteristics of rainfall infiltration and water distribution under different site and vegetation cover conditions. However, there is still a lack of sufficient research on the response process of deep soil moisture to different degrees and scales of precipitation, and research on the soil moisture infiltration process in the Mu Us sandy land only stays at the basic observation level, without conducting simulation predictions. This study analyzed the impact of rainfall on soil water and its replenishment effect on soil water through synchronous monitoring of rainfall and soil moisture content in the Mu Us sandy land. Subsequently, a model was used to fit the changes in soil moisture after each rainfall event [15-20].

1. Experiment site

Table 1: The basic situation of the study area

Stage	Type	Characters in land surface and vegetation	Vegetation coverage (%)
Pioneer stage	Shifting sandy land	The sandy land is covered by sporadic Agriophyllum squarrosum, Psammochloa villosa, Artemisia sphaerocephala krasch and Artemisia Ordosica. The soil is loose with no crust and easy to be eroded.	5-20
Sparse stage	Semi-fixed sandy land	The sandy land is covered by Artemisia Ordosica、Artemisia sphaerocephala krasch and Leymus secalinus. The coverage of crust is about 10%-30%.	20-30
Build phase	Fixed sandy land	The sandy land is covered by Artemisia Ordosica、Suaeda glauca, Setaria viridis and Bassia dasyphylla,The coverage of crust is about 60%-80% with the thickness is 0.5~1.5cm.	30-50

The experiment site is located in the Mu Us Sandy Land and administratively governed by Uxin Banner (County), Inner Mongolian Autonomous Region. The Mu Us Sandy Land (37°26.5′-39°21.5′, 107°20.4′-111°30.3′) is located at an altitude of 1200 to 1600 m, with a gently undulated topography and a total area of about 40,000 km2. The climate is continental semi-arid, with moderate temperature and low rainfall. The long-term average annual precipitation at the experiment site is 341mm per year, about 70% of which occurs between July to September. The mean annual temperature is 8.4 ℃, with a maximum monthly mean temperature of 22 ℃ occurring in July and a minimum of −11°C in January. The Mu Us Sandy Land consists of fixed, semifixed, and shifting sand dunes. The soils covering these sand dunes consist of >90% sand and are thus categorized as sandy soils according to the China Soil Taxonomy System. Natural vegetation at the

site is sandy grassland dominated by Artemisia Ordosica Krasch. In general, the fixed, semi-fixed, and shifting sand dunes are covered by 30% to 50%, 10% to 30%, and <10% vegetation, respectively. Fixed and shifting sand dunes are the two major vegetation landscapes in Mu Us Sandy Land. Fixed sand dunes indicate a slightly degraded ecosystem, and shifting sand dunes suggest a seriously degraded ecosystem. Table 1 shows the vegetation characteristics of different fixed types of sandy land in the study area.

2. Materials and methods

We used AR-5 soil moisture automatic monitoring system for a Long-term and continuous measurement of soil moisture in the site between sand dunes with a slope less than 5o.The system consisted 5 EC-5 detectors and an AR-5 data collector. EC-5 is a soil moisture detector developed by American Decagon Company, which based on the relationship between soil water content and soil dielectric constant. The EC-5 sensor was introduced in 2006 and it was a useful tool to monitor water movement in soil and estimate the water content of sandy soil. The EC-5 sensor was designed to minimize sensitivity to fertilizer-induced salinity, soil temperature variations, and electrical interference in the field. However, EC-5 sensor readings were influenced by temperature changes depending on the dielectric permittivity of the media; thus, such readings should be corrected based on continuous measurements of soil temperature and soil water content. Kizito et al. (2008) evaluated the effects of temperature on the measurement of soil water content by using an EC-TE sensor (which comprises an identical water content measurement circuitry to that of the EC-5) based on a laboratory experiment. The EC-TE sensor exhibited temperature sensitivity of the soil water content of approximately 0.02 m3·m−3 at a change in temperature of 10°C in porous media. Parsons and Bandaranayake (2009) evaluated the performance of the EC-5 sensor with sandy soils in Florida and concluded that this sensor is stable and effective in the field based on the results of a one year experiment. The EC-5 sensor was not sensitive to temperature fluctuations; probe output increases by approximately 1% or approximately 0.0071 m3·m−3 according to the factory calibration equation (Decagon Devices, 2006) when the temperature gradually changes from 3 to 38 ℃. Rosenbaum et al. (2011) found that the EC-5 and EC-TE sensors underestimated permittivity at low temperatures (5–25 ℃) and overestimated this parameter at high temperatures (25–40 ℃); temperature dependence increased as the water volume fraction of the medium increased.

Because most capacitance sensors are sensitive to the variability of soil characteristics, such as bulk density, texture, temperature, and salinity, field-specific calibration provides more accurate measurements than factory calibration. Numerous efforts have been made to calibrate the capacitance of soil moisture sensors, and most of these efforts were based on laboratory experiments using dielectric liquids or repacked soils. Although laboratory calibration is feasible and informative, field calibration has the advantage of incorporating measurement conditions that are difficult to be created in a laboratory, such as the location-specific texture, structure, and bulk density of the target soils. Therefore, Wu Bo et al. (2014) considering soil temperature, soil texture, soil bulk density and other factors calibrated the EC-5 sensor in 2013, the calibrating equation is as follows:

$$C=0.1506-0.001506MV+3.218\ (MV)^{2}$$

where C represents the soil water content (m3·m−3), MV represents the output of the EC-5 sensor readings (m3·m−3). The data of soil water content used in this study were all derived from the field-calibration equation.AR-5 data collector is to provide data storage and power supply for EC-5 sensor. The installation depth of each EC-5 were 10cm, 20cm, 40cm, 60cm,80cm,100cm,120cm, 160cm and 200cm, a total of nine layers. The groundwater level in the study area was generally below 5 meters, so the soil water content of 0-200cm was not affected by

groundwater.

We began to install the instruments in October 2015, and set the pluviometer to monitor the precipitation. In this study, 3 repeated trials were conducted in three different places. From October 2015 to February 2016, it was at the soil disturbance restoration period, the data recorded after March 2016 were used as effective data to analyze the soil moisture dynamics during the growing season. The data were processed by SPSS16.0 and Excel2013, and the mean value was expressed in the form of Mean + SE. The significant difference test (a=0.05) was performed by one-way ANOVA (LSD).

Due to the existing infiltration models having their own applicable conditions and basic characteristics, it is necessary to verify the model before applying it to specific areas. After verifying multiple models, this study ultimately selected a multi chamber model to predict precipitation infiltration in the study area. The expression of the model is:

$$\frac{dx_0(t)}{dt}=-k01x0 \tag{1}$$

$$\frac{dx_1(t)}{dt}=Fk01x0-kx1 \tag{2}$$

$$x0(t) \mid t=0=A0,\ x1(t) \mid t=0=0 \tag{3}$$

Among them, A0 is precipitation, x0 (t) is infiltration, k01 is the rate of water transfer from the absorption chamber to the central chamber, k is the rate of water removal from the central chamber, and 0<F<1 is the effective absorption rate. The solution of the above differential equation is:

$$x0(t)=A0e^{-k_0t} \tag{4}$$

$$x1(t)=\frac{Fk_0A_0}{k_0-k}(e^{-kt}-e^{-k_0t})$$

After solving, the L-M algorithm is used to estimate the parameters of nonlinear regression. Here, let y=g (a, b)+c, where g is a nonlinear function of parameter b (b1, b2, b3...), and a (a1, a2, a3...) is an independent variable. When parameter b cannot be obtained through the least squares method, a step-by-step approximation method is used here. The initial value of parameter vector b is given as c, and the difference between vector b and c is e, that is, b=c+e. Subsequently, by expanding g (a, b) at point c using Taylor's formula, we can obtain:

$$g(a,b)\approx g(a,c)+\frac{dg(a,c)}{dc_1}(c1-c)+\frac{dg(a,c)}{dc_2}(c2-c)+\frac{dg(a,c)}{dc_3}(c2-c)+\cdots\cdots$$

$$= g(a,c)+\frac{dg(a,c)}{dc_1}e1+\frac{dg(a,c)}{dc_2}e2+\frac{dg(a,c)}{dc_3}e3+\cdots\cdots \tag{5}$$

When a takes the given value an, equations 2-5 can be written as:

$$g(an,c)\approx gan+\frac{dg_{a_n}}{dc_1}e1+\frac{dg_{a_n}}{dc_2}e2+\frac{dg_{a_n}}{dc_3}e3+\cdots\cdots \tag{6}$$

When the initial value c and the observed value g (a, b) are determined, then both gan and (dg_ (a_n))/(dc_n) are also determined accordingly. Then, the e value that minimizes the residual Q is obtained using the least squares method. The general calculation formula for the Q value with respect to the values of a, b, c, and e is:

$$Q=\sum_{n=1}^{m}[b_n-g(a_n,c)^{\,2}] \tag{7}$$

$$\approx\sum_{n=1}^{m}[b_n-(g_{a_n}+\frac{dg_{a_n}}{dc_1}\mathrm{e}_1+\frac{dg_{a_n}}{dc_2}\mathrm{e}_2+\frac{dg_{a_n}}{dc_3}\mathrm{e}_3+\cdots\ldots)]2$$

The derivative of Q with respect to c is:

$$\frac{dQ}{dc_n}=\sum_{n=1}^{m}[b_n-(g_{a_n}+\frac{dg_{a_n}}{dc_1}\mathrm{e}_1+\frac{dg_{a_n}}{dc_2}\mathrm{e}_2+\frac{dg_{a_n}}{dc_3}\mathrm{e}_3+\cdots\ldots)]2(-\frac{dg_{a_n}}{dc_n}) \tag{8}$$

From equations 2-8, it can be seen that if we want to minimize Q, we should make $\frac{dQ}{dc_n}$=0. Therefore, we can obtain the linear equation system about e as follows:

$$\begin{aligned}
&x11e1+x12e2+x13e3\ldots\ldots=x1z\\
&x21e1+x22e2+x23e3\ldots\ldots=x2z\\
&\quad\vdots\\
&xn1e1+xn2e2+xn3e3\ldots\ldots=xnz
\end{aligned} \tag{9}$$

The following conditions are met:

$$xmn=\sum_{n=1}^{m}\frac{dg_{a_n}}{dc_1}\frac{dg_{a_n}}{de_1} \tag{10}$$

$$amz=\frac{dg_{a_n}}{de_1}(bn-gan)$$

According to the above equation, the value of e can be calculated to obtain an approximate estimate of parameter c. To reduce errors, it is necessary to repeatedly introduce and verify to determine accuracy.If the G-N method is used to solve equations 2-9, damping factors need to be added γ, Thus, the following equation system is obtained:

$$\begin{aligned}
&(x11+\gamma)e1+x12e2+x13e3\ldots\ldots=x1z\\
&x21e1+(x22+\gamma)e2+x23e3\ldots\ldots=x2z\\
&\quad\vdots\\
&xn1e1+xn2e2+(xn3+\gamma)e3\ldots\ldots=xnz
\end{aligned} \tag{11}$$

During the calculation process, γ The value of will change with the introduction process, and the calculation steps are as follows: ① Given the initial value of the parameter c to be estimated, calculate Q, and provide the damping factor γ The scaling constant s (usually greater than 1) is then adjusted according to s γ The value range of; ② When iterating, it is possible to γ= si γ 0, where i is the minimum value it can take to obtain the value of e to minimize Q; ③ hold γ, s. Replace the current value of Q with the formula and proceed to the next iteration until e cannot be smaller. When using the G-N method for estimation, a given initial value is required, which has a significant impact on the convergence rate. Generally speaking, the initial values can be obtained from research records. When using the multi chamber model in the vertical direction of soil moisture dynamics, it is assumed that the wetting front is a straight line, and the two parts before and after the wetting front are simplified into two extreme distribution characteristics: fully saturated and completely in the initial soil moisture state. In order to more accurately describe the distribution pattern of soil moisture content, the moisture content after the wetting front can be fitted as a straight line A1 (x1), and the moisture content before the wetting front can be fitted as a straight line A2 (x2). The intersection point of the two lines is the critical moisture content A0, and it is assumed that the critical moisture content does not change at any time, and the slope of the straight line A2 (x2) does

not change with time. An expression for cumulative infiltration was proposed:

$$I= [\frac{A_0+A_s}{2}-A_i] (x-xf+x0) +\frac{(A_0-A_i)(x_f-x_0)}{2} \quad (12)$$

Among them, I is the cumulative infiltration amount (mm); A0 is the critical moisture content (%); As is the saturated water content (%); Ai is the initial soil moisture content (%); X is the advancing distance of the moist front (cm); Xf and x0 are the coordinates (cm) of the front and rear ends of the wetting front, respectively. The formula for calculating the infiltration rate i obtained by taking the derivative of the cumulative infiltration amount I with respect to time t is:

$$i= [\frac{A_0+A_s}{2}-A_i]\frac{dx}{dt} \quad (13)$$

Equations 2-13 indicate that as long as the relationship curve between infiltration depth and time is obtained, the law of infiltration rate changing with time can be obtained. When precipitation infiltrates to a certain extent, the soil moisture content of the soil layer before and after the wetting front basically reaches an equilibrium state, which can be represented by the following equation:

$$\lim_{h\to x}(S-T)=0 \ \rightarrow \ \lim_{h\to x} S=T \quad (14)$$

Among them, x is the soil depth, h is the maximum value of soil infiltration depth, S is the soil moisture content before the wetting front, and T is the soil moisture content after the wetting front.When the precipitation infiltration process is represented by a multi chamber model, the equation is:

$$\frac{dS_1}{dx}=-iS1 \quad (15)$$

$$\frac{d(S-T)}{dx}=iS1-i(S-T) \quad (16)$$

$$S \mid x=0=S0 \quad (17)$$

By solving the above differential equation, the vertical variation equation of soil moisture can be obtained as follows:

$$S=ae-ix-ce-jx+T \quad (18)$$

Among them, x is the depth of soil infiltration, S is the supplementary water, i is the rate of soil moisture absorption, j is the rate of soil moisture evaporation, a and c are normal numbers, and S0=a-c+T. Transforming the expressions for cumulative infiltration amount and infiltration rate, the following equation is obtained:

$$I=\sum_i(x_i-x_0) \ \triangle x \quad (19)$$

$$i=\frac{K_s h_d}{n(x_s-x_r)}\frac{dK}{dx}=\frac{x_i-x_0}{\triangle x}\frac{K_s h_d}{n(x_s-x_r)}$$

The expression of the model can be corrected to:

$$\frac{dS_1}{dx}=-iS1\ln x$$

$$\frac{d(S_1-|S-T|)}{dx}=-j(S1-|S-T|) \quad (20)$$

$$\frac{d}{dx}(K_x\frac{dg}{dx})=\frac{d}{dx}(-\frac{d}{dx}x^{\frac{m-n-1}{n}}\frac{K_x h_d}{n})$$

The solution of the equation system is:

S1=ae-ix(lnx-1)

(21)

S1-｜S-T｜=ce-jx(a, i, c, j＞0)

Among them, P is the replenishment of soil moisture by precipitation, and IS is the initial soil moisture content. The replenishment of soil moisture by precipitation is significantly correlated with precipitation and precipitation intensity. The relationship between soil moisture increment and precipitation and precipitation intensity can be expressed as follows:

$$\frac{dW}{d(y-b)} = \frac{gce^{hln(y-b)}}{y-b} \tag{22}$$

In the equation, W is the change in soil moisture content of a specific soil layer caused by precipitation, y is the precipitation (mm), b is the minimum effective precipitation, y-b is the theoretical effective precipitation, and g and h are fitting parameters. The solution of the above differential equation is:

W=g(y-b)h (23)

Equations 2-23 reflect the proportion of effective precipitation and precipitation intensity converted into soil moisture, therefore g and h indirectly reflect the conversion rate of effective precipitation. From equations 2-22 and 2-23, it can be seen that precipitation less than effective precipitation does not have a significant impact on the change in soil moisture content of the corresponding soil layer. If the replenishment of soil moisture is recorded as S1, then there are:

S1=IS+P (24)

The consumption of soil moisture is S1-S. During the process of precipitation infiltration, S1 will decrease with the increase of soil depth, and there are:

$$\lim_{x\to h} S_1 = 0 \tag{25}$$

According to previous empirical formulas, the trend of S1 change is directly proportional to lnx, denoted as ilnx; The trend of S changes tends to stabilize with changes in soil depth, and there are:

$$\lim_{x\to h} S - T = 0 \tag{26}$$

Transforming equations 2-20 yields:

$$\frac{dS}{dx}=\frac{1}{\Gamma(1-x)}\int_0^T \frac{da}{(t-a)^b}=\frac{1}{\Gamma(1-x)}\int_0^t \frac{dc}{da}\frac{1}{(1-x)^{lnb}}\frac{1}{r_s-r_0} \tag{27}$$

If considering the problem of horizontal infiltration, the equation is:

$$S0= (1- \frac{ax^{\frac{n}{m-n-1-i}}}{T}) (Sa+Sc) +Sr \tag{28}$$

By introducing equations 2-19, the cumulative infiltration amount can be obtained as:

$$I=\frac{(Sa+Sc)\,(m-n-1)}{m-i-j}x_t - (r_s - r_0)\,x_t \tag{29}$$

The soil moisture flux at this time is:

$$Q=\frac{K(h)dh}{dx} = \frac{x^{\frac{n}{m-n-1-i}}}{aK^2h_d}(1-\frac{ax}{x_t})\ lnx^{\frac{n}{m-n-i-1}}\frac{1}{x_t} \tag{30}$$

Using the Caputo order derivative difference approximation method to solve, and using the

center difference method for spatial derivatives, the basic equation at point A is:

$$\text{Drj}=\frac{(\triangle b)^{-a}}{\Gamma(1-\text{a})}\left[\sum_{i=1}^{n-1} a_{n-k-1}+ce^{jx}+Tc_{n-k}+\frac{dr}{dx}\Gamma(2-a)\right] \quad (31)$$

$$\frac{d}{dx}\left(\text{D}\frac{da}{dx}\right)=\frac{D_{j+\frac{1}{2}}^{n}\left(r_{j+1}^{n}-r_{j}^{n}\right)-D_{j-\frac{1}{2}}^{n}\left(r_{j}^{n}-r_{j-1}^{n}\right)}{(\triangle x)^{2}} \quad (32)$$

The expression for organizing S is:

$$\text{S= ae-ix(lnx-1)- ce-jx +T(a, c belong to real number, i, j}>0) \quad (33)$$

This equation considers the effects of factors such as precipitation, root system, soil properties, and initial soil moisture content on the infiltration process, which can better simulate the precipitation infiltration process. Moreover, the replenishment rate of soil moisture in equations 2-18 is a constant, while in equations 2-33 it is a variable, which is more in line with the actual situation.

3. Results

3.1 Precipitation characteristics in the study area

A total of 41 rainfall events occurred in the research area in 2014, with a total precipitation of 342.25mm. Among them, the growth season occurred 35 times, with a precipitation of 332.75mm, accounting for 97.2% of the annual precipitation. Most of the precipitation in the research area is mainly from light to moderate, with 28 occurrences of precipitation less than 10mm. The frequency of precipitation accounts for 67% of the total annual precipitation, but the precipitation only accounts for 18.19% of the annual precipitation; There were 10 occurrences exceeding 10mm, with a precipitation of 266.35mm, accounting for 80.05% of the precipitation during the growing season; There were 5 times when the precipitation exceeded 20mm, with a precipitation of 173.15mm, accounting for 52.2% of the precipitation during the growing season. During the growth season, precipitation is most concentrated from July to September, accounting for 79.6% of the growth season (Figure 1, Figure 2). The distribution of rainfall intensity in 41 rainfall events is shown in Figure 3. The frequency of rainfall intensity less than 2.5 mm/h exceeds 80%, and only about 1% of rainfall intensity exceeds 15 mm/h. This indicates that precipitation in the study area is basically absorbed by the soil or lost through evapotranspiration, and generally does not form surface runoff.

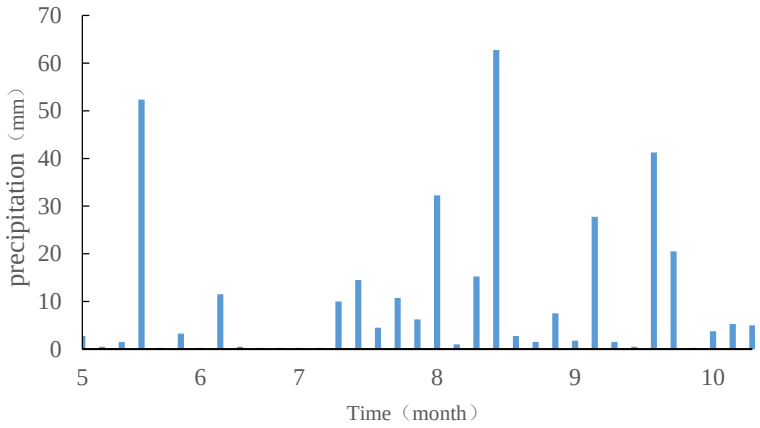

Figure 1: The rainfall in the growing season

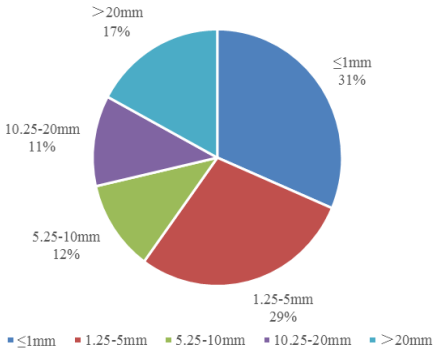

Figure 2: The distribution of precipitation in the growing season

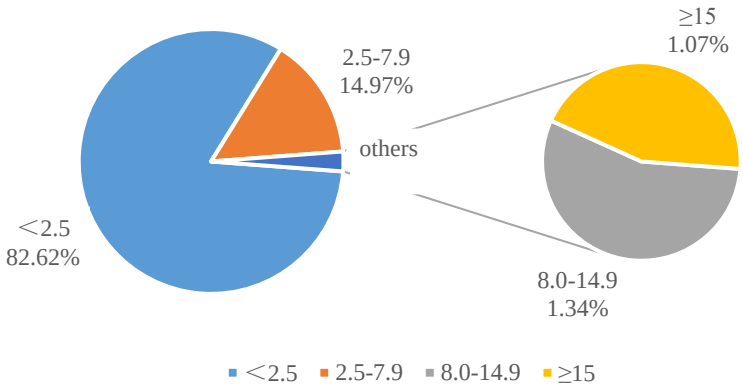

Figure 3: The distribution of rainfall intensity (mm/h)

3.2 Relationship between initial soil moisture content and rainfall infiltration

During the research period, the minimum values of soil moisture content in each layer of 10-200cm appeared in early August. And since May, the overall soil moisture content has been in a relatively low state. The precipitation that began on May 19th (lasting 56 hours) significantly affected the soil moisture content at 10-80cm. Due to the absence of any precipitation events for a long period of time and the long duration of this precipitation, with an average precipitation intensity greater than 0.9mm/h, this precipitation can be used as a typical representative to analyze the relationship between precipitation and infiltration depth, wetting front and fluctuation peak value when the soil moisture content before precipitation is low, as well as the response process of soil moisture to precipitation. The maximum soil moisture content of each layer occurs at the end of August, and during this period, the soil moisture content has remained relatively high overall. Due to frequent precipitation and overall high soil moisture content, the duration of this precipitation (lasting for 81 hours) is the annual maximum. Therefore, this precipitation can be regarded as a typical precipitation event. Analyze the relationship between precipitation, precipitation duration, infiltration depth, and fluctuation peak when the soil moisture content is high before precipitation, and further explore the response process of soil moisture to precipitation. Table 2 records the initial soil moisture content before the two precipitation events, and it can be seen from the table that there are significant differences in the initial soil moisture content before the two precipitation events. Except for the 160cm and 200cm layers, the soil moisture content before the precipitation on August 20th was significantly higher than that before the precipitation on May 19th.

Table 2: Initial soil moisture content before two precipitation events (%)

Time	Soil depth								
	10cm	20cm	40cm	60cm	80cm	100cm	120cm	160cm	200cm
5.19	6.47	6.03	5.75	5.34	6.03	6.37	6.15	6.75	9.36
8.20	13.04	12.28	14.12	12.89	13.17	12.41	12.31	3.14	3.87

Figure 4 shows the relationship between infiltration depth, fluctuation peak, cumulative precipitation, and precipitation time in a fixed sandy land when the initial soil moisture content is low. The precipitation began at 10:00 on May 19th (recorded as 0h), lasting for 56 hours, with a cumulative precipitation of 52.35mm. The precipitation from 0-47h was 43.14mm, and from 49-58h was 9.21mm. The average soil moisture content from 0-200cm before the precipitation was 5.46%. Starting from May 20th, there was a peak fluctuation in soil moisture content at 10-40cm. There was no significant change in soil moisture content in soil layers below 80cm. The analysis of this precipitation infiltration shows that the time required for the soil infiltration wetting front to reach the 10cm, 20cm, 40cm, 60cm, and 80cm layers is 6h, 10h, 27h, 48h, and 69h, respectively, with corresponding precipitation amounts of 9.85mm, 14.97mm, 31.24mm, 43.14mm, and 52.35mm. In this precipitation, the soil layer of 100-200cm was not affected by this precipitation. This indicates that when the initial soil moisture content is low, the infiltration depth of 52.35mm precipitation exceeds 80cm and is less than 100cm. However, previous research by Liu Xinping et al. (2006) in the Mu Us sandy land showed that precipitation less than 14.2mm would be absorbed by the surface soil or lost through evapotranspiration, and the infiltration depth after redistribution of precipitation would not exceed 60cm. In addition, the monitoring data of this study shows that the five precipitation events of less than 14.2mm that occurred from May to August only caused changes in soil moisture content at a depth of 10-40cm. Therefore, the analysis suggests that the 9.21mm precipitation occurring from 49-58h can be considered as having no significant impact on soil layers of 60cm and below, while the 43.14mm single precipitation wetting front occurring from 0-47h is 80cm.

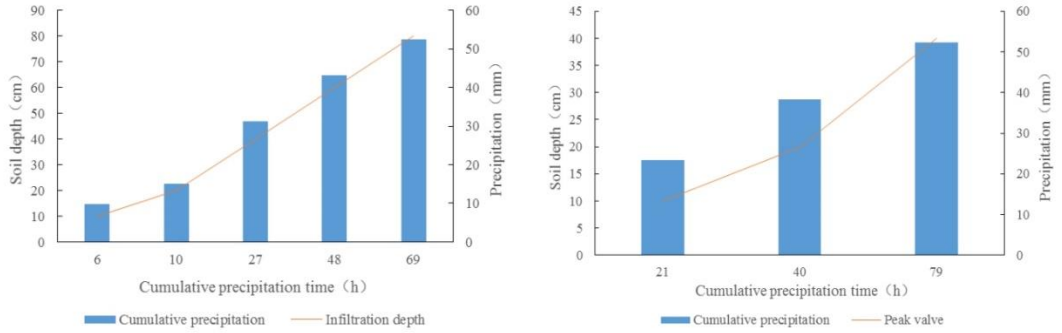

Figure 4: Infiltration at Low Initial Soil Moisture Content

Generally speaking, the infiltration of soil moisture under saturated conditions is called saturation infiltration. However, under the combined influence of factors such as precipitation intensity and evapotranspiration, larger precipitation may not necessarily generate saturated infiltration. However, the conditions for saturated infiltration to occur are very special and not significantly related to precipitation, only influenced by precipitation intensity. Research has shown that the infiltration of soil moisture is still in an unsaturated state when it is less than 12mm/h in the Mu Us sandy land. The monitoring results of soil moisture content indicate that the maximum value of soil moisture content was only maintained for 3 hours at most, indicating that the soil moisture

content only reached saturation in a short period of time, and remained in an unsaturated infiltration state for most of the remaining time. The peak fluctuation mentioned in this article is the maximum value that soil moisture can reach after a single precipitation.

Figure 5 shows the relationship between infiltration depth, fluctuation peak, cumulative precipitation, and precipitation time when the initial soil moisture content is high in a fixed sandy land. The precipitation began at 14:00 on August 20th (recorded as 0h), lasting for 81 hours, with a cumulative precipitation of 62.75mm and an average precipitation intensity of 0.75mm/h. However, due to the precipitation intensity exceeding 13.6 mm/h in the first 2 hours of the precipitation process, surface runoff occurred in some areas. The precipitation from 0-54 hours is 48.37mm, from 57-79 hours is 10.73mm, and from 81-96 hours is 3.6mm. The average soil moisture content from 0-200cm before precipitation is 10.37%. The precipitation that began on August 20th (lasting for 81 hours) had a significant impact on the soil moisture content at a depth of 120cm in the fixed sandy land, and there was no significant change in the soil moisture content below 120cm. From Figure 5.4, it can be seen that the required precipitation and time for the moist front to reach 10cm, 20cm, 40cm, 60cm, 80cm, 100cm, and 120cm are 6.14mm (4h), 8.75mm (5h), 24.18mm (17h), 32.31mm (35h), 42.75mm (40h), 44.25mm (51h), and 51.72mm (63h), respectively. This indicates that the infiltration depth of 62.75mm precipitation is greater than 120cm, but less than 160cm. However, according to previous research conclusions and analysis of the previous precipitation, the infiltration depth after redistribution of precipitation at 57-79h and 81-96h did not reach 60cm. Therefore, it can be considered that when the initial soil moisture content is high, the infiltration depth of precipitation at 48.37mm in a single field is between 120-160cm.

From Figure 5, it can be seen that the cumulative precipitation and time corresponding to the peak fluctuation at 10cm (17.39 ± 0.12) %, 20cm (16.43 ± 0.19)%, and 40cm (17.11 ± 0.19)% are 23.44mm (21h), 38.31mm (40h), and 52.35mm (79h), respectively. The difference in soil moisture content at the peak fluctuation is extremely significant compared to before precipitation. This result indicates that precipitation from 0-47 hours can bring fluctuation peaks to soil moisture from 0-20 cm, and the fluctuation peak at 40 cm needs to be reached after accumulating 9.21 mm of precipitation.

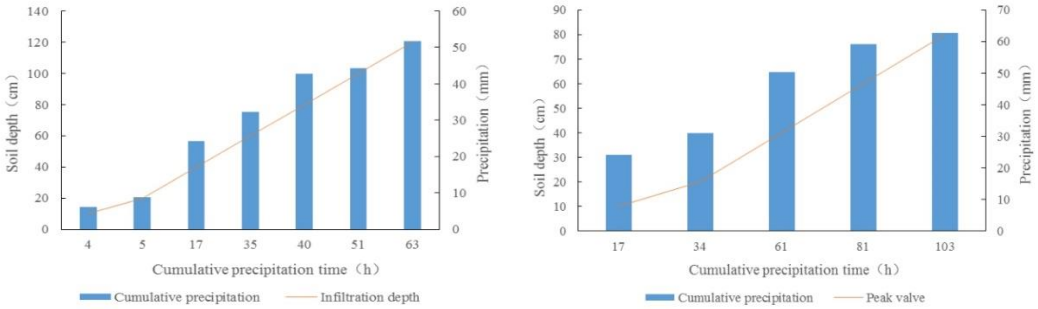

Figure 5: Infiltration situation at high initial soil moisture content

3.3 Precipitation infiltration fitting

The colormap function and shading interp function in Matlab were used to fit the infiltration of two precipitation events, and the fitting results are shown in Figure 6. The revised model was validated using measured data, and the validation results are shown in Table 3. From the table, it can be seen that all parameters of the modified model are within the allowable range, with R2 above 0.8, indicating that the modified model reasonably simulates the infiltration process.

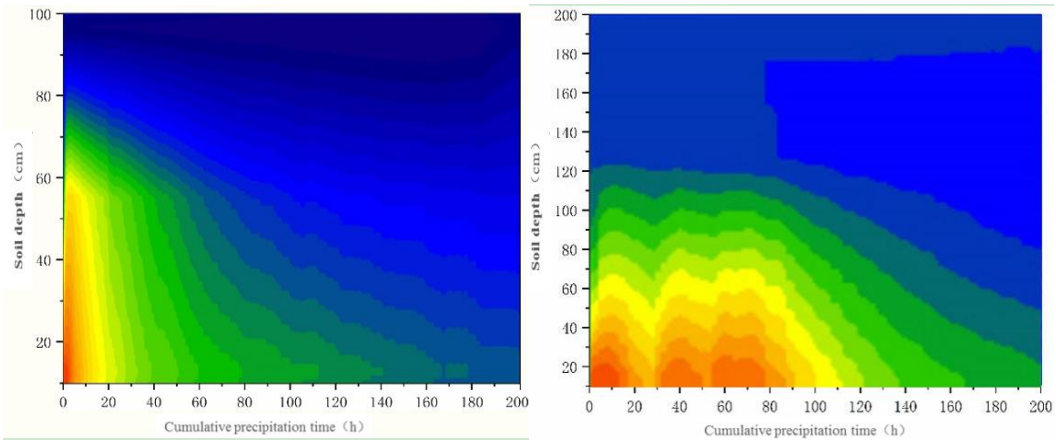

The first precipitation The second precipitation

Figure 6: Fitting Diagram of Precipitation Infiltration

Table 3: Model fitting results

Time	Fit parameters					R^2
	i	j	T	a	c	
5.19	3.145	2.312	11.63	0.188	1.085	0.933
8.20	3.531	3.522	8.465	-0.879	-0.870	0.871

The infiltration fitting data in 8 precipitation days (light rain, moderate rain, heavy rain and rainstorm) of the same year can be divided into 3 groups, and the grouping results are shown in Table 4. The main basis for grouping is the initial soil moisture content, root biomass, precipitation, and precipitation intensity. The main difference between the three types of sample plots is the grouping of heavy rain and rainstorm. The two light and moderate rains are in the first group. When the combined effect of precipitation and precipitation intensity (replenishment of soil water) reaches 28.45mm, a situation of 0.01>c-a>0 occurs; When the replenishment of soil water by precipitation ranges from 12.35 to 28.45mm, the corresponding parameter standard is c-a>0.01; When the replenishment of soil water by precipitation is less than 12.35mm, the corresponding parameter standard is c<a<0.

Table 4: Classification of Monitoring Data

Group	parameter value	date
1	c＜a＜0	6.8, 9.4, 6.14, 8.28
2	c-a＞0.01	7.10, 9.3, 5.19
3	0.01＞c-a＞0	8.20

With the increase of vegetation coverage, soil stability has significantly improved, and the range of parameter values representing precipitation infiltration rate shows a clear trend of change. From the parameter range of the differential equation, it can be seen that as vegetation coverage increases, the soil surface area in contact with water droplets gradually decreases; The higher the flow rate of precipitation on the soil surface, the smaller the positive pressure formed by the water layer on the soil surface, resulting in a decrease in infiltration capacity. In addition, when the amount and intensity of precipitation are the same, the higher the vegetation coverage, the smaller the actual rainfall bearing capacity per unit area of soil, which also leads to a decrease in infiltration rate.

Based on the monitoring data of two precipitation events, images of precipitation infiltration over time can be obtained, which can more intuitively demonstrate the relationship between simulated and monitored values. If the sample land type is extended to three types: fixed sand land,

semi fixed sand land, and mobile sand land, this model can also well reflect the infiltration process. Figure 7 shows the relationship between the fitting curves and measured values of two precipitation events under different initial soil moisture contents. The monitoring of soil moisture is conducted every half hour, and the scatter points in the data that show a significant difference in soil moisture content at a certain time before and after measurement are represented by increasing. From the image, it can be seen that the fitted curve after parameter correction has a higher R value compared to the measured results, indicating that the modified model can better fit the precipitation infiltration situation. From the graph, it can also be seen that the regression functions formed by the fitting curves and measured values of the three types of plots have certain patterns.

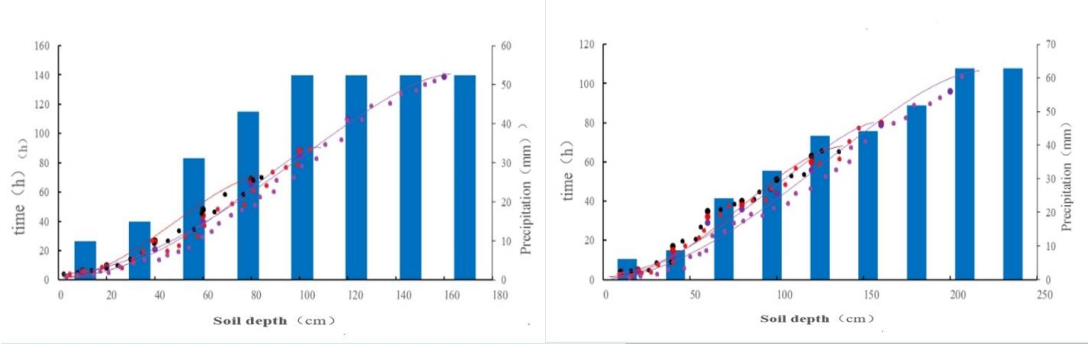

Figure 7: Relationship between Two Precipitation Fitting Curves and Measured Values

4. Conclusion

(1) The cumulative precipitation during the growth season in the research area is 332.75mm, which has a significant impact on the soil moisture content of the 0-120cm soil layer. The precipitation before August only affects 80cm and above; The precipitation from August to October has a significant impact on the soil moisture content of the 0-120cm soil layer.

(2) After each precipitation event, there will be significant changes in the soil moisture content of 0-60cm layers in various fields. After each precipitation, the maximum water content of the surface soil is significantly higher than that of the deep soil. Due to significant differences in the initial soil moisture content before the second precipitation, the maximum soil moisture content after the second precipitation is significantly higher than that after the first precipitation. The initial soil moisture content has a significant impact on infiltration and redistribution, resulting in a significant difference in the migration rate of the wetting front and the maximum soil moisture content after precipitation.

(3) The multi compartment model is used to simulate the precipitation infiltration, and the parameters are modified after the preliminary validation of the model. The results show that the modified model parameters meet the set value range, the Goodness of fit meets the statistical requirements, and the modified model can better reflect the infiltration in different areas with different precipitation amounts, different precipitation intensities. According to the different parameter ranges in the improved model, it can express the relationship between plants and soil moisture under different precipitation conditions and different time periods.

References

[1] Feng Q. Advance in Sandy—land Moisture Research [J]. Journal of Desert Research, 1993, 13(2):9-13.
[2] Xiao D. Comments on the progress and direction in soil water research [J]. Ecology & Environmental Sciences, 2009, 18(3):1182-1188.
[3] AN Hui, AN Yu. Soil moisture dynamics and water balance of Salix psammophila shrubs in south edge of Mu Us Sandy Land. Chinese Journal of Applied Ecology [J]. Sep. 2011, 22(9): 2247 —2252.

[4] Cui Liqiang, Wu Bo, et al. The characteristics of soil water in different vegetation coverage on the southeastern margin Mu us sandy land. Journal of Arid Land Resources and Environment [J]. 2010, 24(2):177-182.
[5] Dong D G, Bo W U, Jun C L, et al. Present Situation, Cause and Control Way of Desertification in China [J]. Journal of Desert Research, 1999.
[6] Chao-Feng F U, Zhao J B. Distribution of Soil Moisture Content in Different Types of Sand Dunes in the Southeastern Marginal Zone of the Mu Us Sandy Land [J]. Arid Zone Research, 2011, 28(3):377-383.
[7] Guo K., Dong X. J., & Liu Z. M. (2000). Characteristics of soil moisture content on sand dunes in Mu us sandy grassland: why Artemisia Ordosica declines on old fixed sand dunes. Acta Phytoecologica Sinica, 2000, 24:275-279.
[8] Guo K. Cyclic succession of Artemisia ordosica Krasch community in the Mu Us sandy grassland [J]. Acta Phytoecologica Sinica [J]. 24(2): 243—247, 2000.
[9] Zhibin H E, Zhao W Z. Variability of Soil Moisture of Shifting Sandy Land and Its Dependence on Precipitation in Semi-arid Region [J]. Journal of Desert Research, 2002, 22(4):359-362.
[10] Bao H, Hou L, Shen J, et al. Research on soil water dynamics of farmland in Mu Us Sand Land [J]. Chinese Journal of Eco-Agriculture, 2014.
[11] Angusa J F, Gault R R. Soil water extraction by dryland crops, annual pastures, and Lucerne in South-eastern Australia. Australian Journal of Soil Research [J]. 2001, 52:183-192.
[12] Brown K W, Evans G B. Increased soil water retention by mixing horizons of shallow sandy soil. Soil Science [J]. 1985, 139:118-121.
[13] Jiang L N, Lu Q, Yang W B, et al. The promoting effect of vegetation recovery after establishment of Poplar fixing sand forest belts in the Horqin Sandy Land of Northeast China. Journal of Food, Agriculture &Environment[J]. 2013, 11(3 &4):2510-2515.
[14] Li X R, Kong D S, Tan H J, et al. Changes in soil and in vegetation following stabilization of dune in southeastern fringe of the Tengger Desert, China. Plant and Soil [J]. 2007, 300:221-231.
[15] Simmons M T, Archer S R, Teague W R, et al. Tree (Prosopis glandulosa) effects on grass growth: An experimental assessment of above-and below ground interactions in a temperate savanna. Journal of Arid Environments [J]. 2008, 72(4):314-325.
[16] Wang X, Chen F H, Dong Z, et al. Evolution of the southern Mu Us Desert in North China over the past 50 years: An analysis using proxies of human activity and climate parameters. Land Degradation & Development [J]. 2004, 15:1-16.
[17] Wu B, Han H Y, He J, et al. Field-specific calibration and evaluation of EC-5 sensor for Sandy soils. Soil Science Society of America Journal [J], 2014, 78:70-78.
[18] Parsons L R, Bandaranayake W M. Performance of a new capacitance soil moisture probe in a sandy soil. [J]. Soil Science Society of America Journal, 2009, 73(4):1378-1385.
[19] Kizito F, Campbell C S, Campbell G S, et al. Frequency, electrical conductivity and temperature analysis of a low-cost capacitance soil moisture sensor [J]. Journal of Hydrology, 2008, 352(3–4):367-378.
[20] Rosenbaum U, Huisman J A, Weuthen A, et al. Sensor-to-sensor variability of the ECH2O EC-5, TE, and 5TE sensors in dielectric liquids. [J]. Vadose Zone Journal, 2010, 9(1): 181-186.